



Quantum simulations of helium clusters with ionic and open shell dopants

Marius Lewerenz

► To cite this version:

Marius Lewerenz. Quantum simulations of helium clusters with ionic and open shell dopants. 2013. ⟨hal-00832918⟩

HAL Id: hal-00832918

<https://hal.science/hal-00832918v1>

Submitted on 11 Jun 2013

HAL is a multi-disciplinary open access archive for the deposit and dissemination of scientific research documents, whether they are published or not. The documents may come from teaching and research institutions in France or abroad, or from public or private research centers.

L'archive ouverte pluridisciplinaire **HAL**, est destinée au dépôt et à la diffusion de documents scientifiques de niveau recherche, publiés ou non, émanant des établissements d'enseignement et de recherche français ou étrangers, des laboratoires publics ou privés.



HAL Authorization

Quantum simulations of helium clusters with ionic and open shell dopants

Marius Lewerenz

Laboratoire de Modélisation et Simulation Multi Echelle
UMR8208 CNRS

Université Paris Est (Marne la Vallée)
5, Blvd. Descartes, Champs sur Marne
77454 Marne la Vallée Cedex 2
France



Acknowledgments

Paris-Est:

Mirjana Mladenović, $\text{CO}^+ @ \text{He}_n$

Ji Jiang, Ph.D student, $\text{Ar}^+ @ \text{He}_n$, $\text{I}^q @ \text{He}_n$

Prague:

Petr Slavíček, $\text{Pb}^{q+} @ \text{He}_n$

What makes helium clusters interesting?

- Helium-helium interaction is of **weak van der Waals** type, closed shell atoms of very low polarisability, $D_e \approx 7.6 \text{ cm}^{-1}$
- Helium atoms have a relatively small mass.
- Large zero point energy effects (D_0 for $\text{He}_2 \approx 0.001 \text{ cm}^{-1}$).
- Helium clusters are small chunks of a quantum liquid.
- Quantum statistical effects: **bosonic** ^4He , fermionic ^3He .
- **Superfluidity** in bulk liquid ^4He below 2.17 K, in ^3He at mK level
- **A very special solvent: Is there a new chemistry?**
- Implantation of dopants through (multiple) inelastic collisions.
- Weak interactions with dopant.
- Binding energy and position of dopants depend on quantum effects.

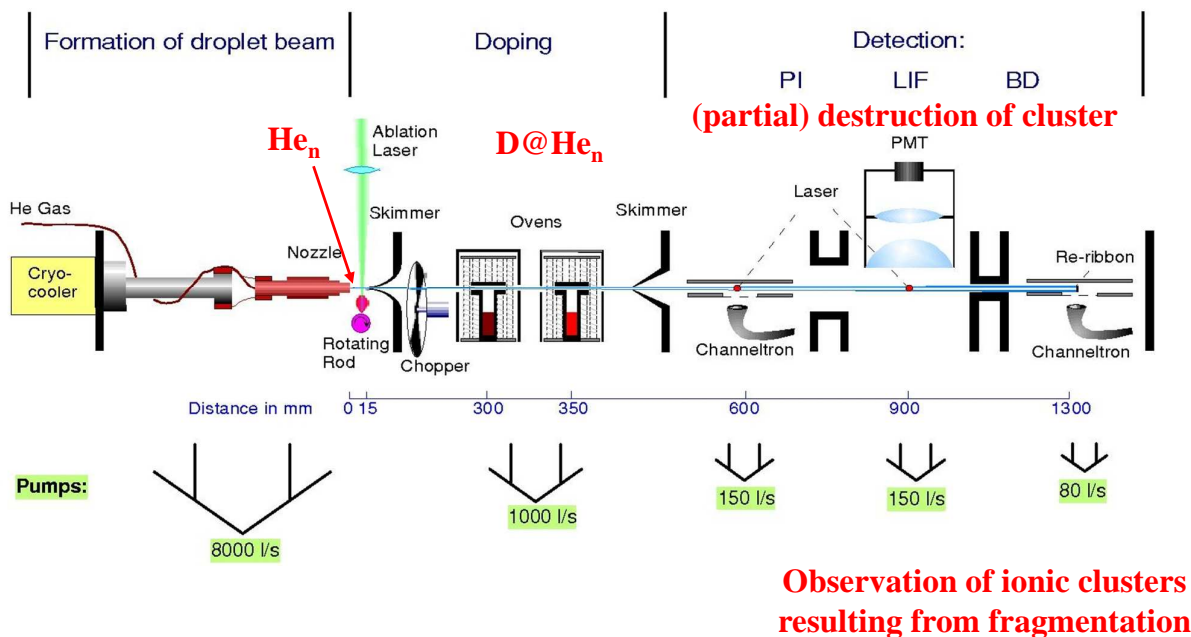
Delicate balance between potential and quantum kinetic energy

Plenty of interesting experiments but theoretical difficulties!

Recent applications of helium clusters

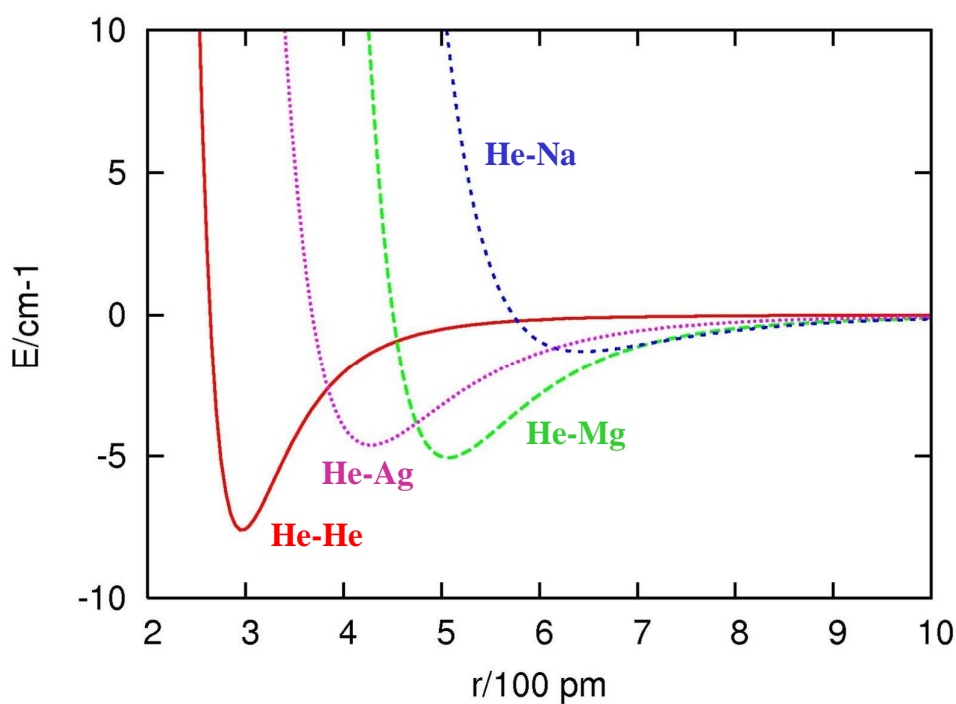
- Matrix spectroscopy with minimal perturbations: **OCS, $(\text{HF})_n$, biomolecules at 0.4 K, radicals**
- Reaction dynamics at very low temperatures: **$\text{Ba} + \text{N}_2\text{O} \rightarrow \text{BaO} + \text{N}_2$**
- Preparation of reactive intermediates: **$\text{HF} \cdots \text{CH}_3$, $\text{HCN} \cdots \text{CH}_3$ etc.**
- Preparation of high spin metal polymers: **Na_3 , K_3 , Rb_3 etc.**
- Assembly of cold clusters: **Ag_n , Mg_n**
- Thermodynamically unstable isomers: **linear $(\text{HCN})_n$**
- Nanomodels for molecule-surface interactions: **$\text{HCN} \cdots \text{Mg}_3$ etc.**
- Container for soft ionisation for analytical mass spectrometry?
- Energy dissipation by coupling to the bath?
- Confinement medium for cluster ignition and Coulomb explosion.
- Spacer for interatomic Coulombic decay (ICD).

A typical helium droplet experiment



Pair potentials involving helium and metals

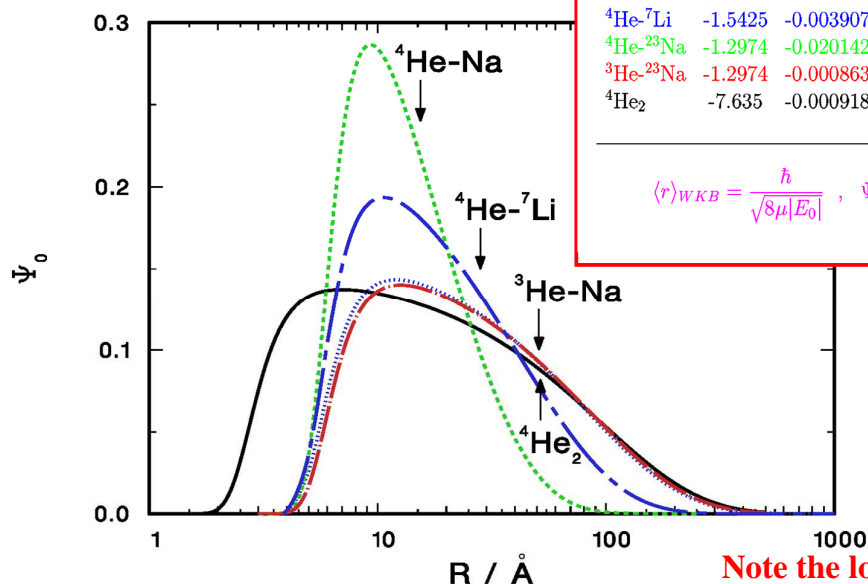
Shallower well than **He-He** and larger equilibrium distance for He-M



Alkali-helium dimers

Variational calculations with large basis sets of Laguerre functions, PRL 1999

All alkali-helium dimers appear to possess a single bound state but are yet unobserved



	V_{min}	E_0	r_{min}	$\langle r \rangle$	$\langle r \rangle_{WKB}$	$\langle T \rangle$
$^4\text{He}-^6\text{Li}$	-1.5425	-0.001053	6.16	48.53	40.80	0.033457
$^4\text{He}-^7\text{Li}$	-1.5425	-0.003907	6.16	28.15	20.56	0.063601
$^4\text{He}-^{23}\text{Na}$	-1.2974	-0.020142	6.43	15.41	7.83	0.125440
$^3\text{He}-^{23}\text{Na}$	-1.2974	-0.000863	6.43	50.85	42.79	0.027745
$^4\text{He}_2$	-7.635	-0.000918	2.97	51.68	47.89	0.069649

$$\langle r \rangle_{WKB} = \frac{\hbar}{\sqrt{8\mu|E_0|}}, \quad \Psi = \exp ikr, \quad k \approx \frac{\sqrt{2\mu E_0}}{\hbar}$$

Predicted to be extremely weakly bound and diffuse

Relevance for BEC?

Note the log scale!

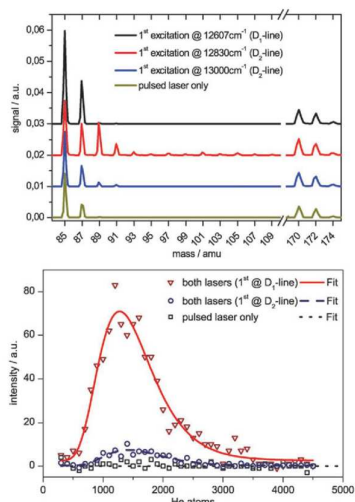
Marius Lewerenz

Strasbourg, 12.7.2012

7

Ions in helium clusters

- Massive change of interaction potential
- Polarisation forces
- Enhanced localisation of helium atoms
- “Snowball” formation



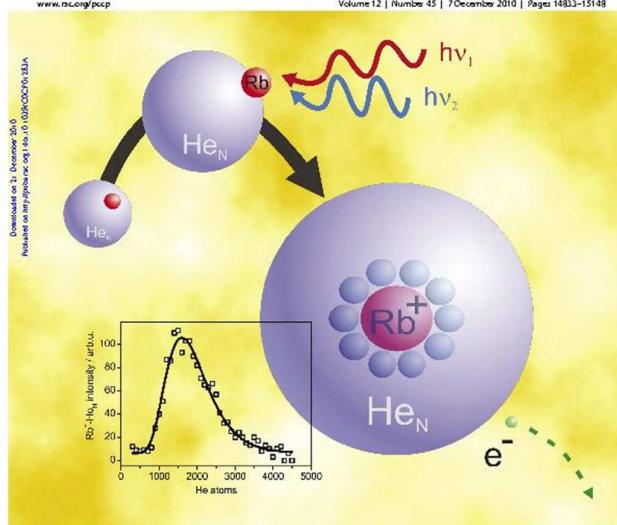
PCCP

Two step photoionisation
Theisen et al., TU Graz

Physical Chemistry Chemical Physics

www.rsc.org/pccp

Volume 12 | Number 45 | 7 December 2010 | Pages 14833–15148



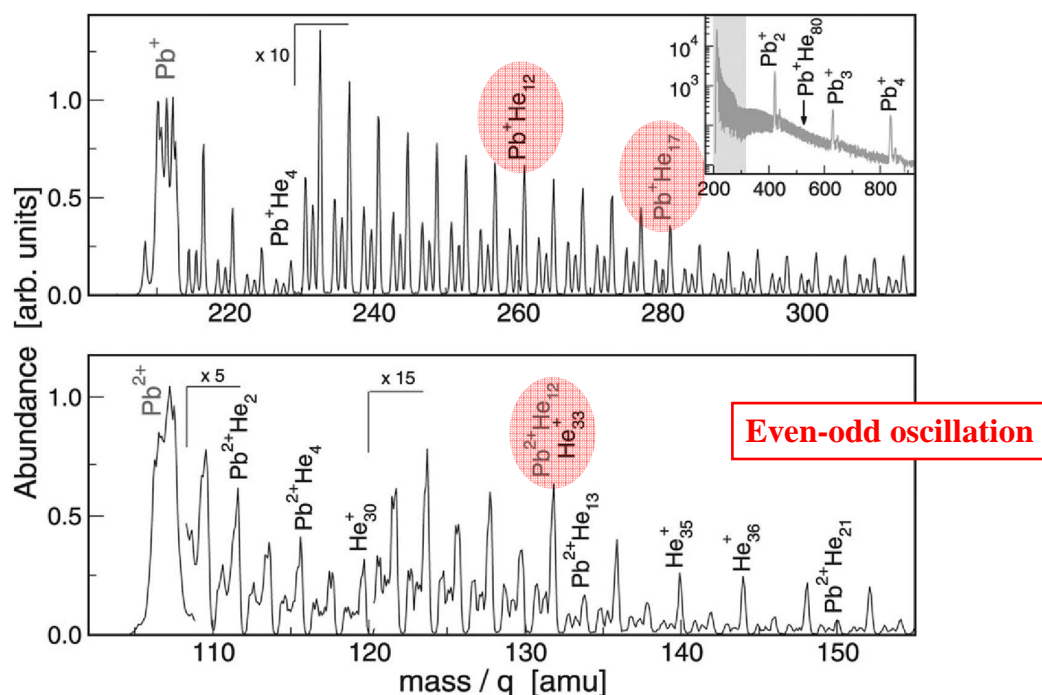
Marius Lewerenz

Strasbourg, 12.7.2012

8

Pb^{q+}He_n mass spectra after fs pulse ionisation

Lead atoms in very large He clusters, Döppner et al. 2007, U. Rostock



Marius Lewerenz

Strasbourg, 12.7.2012

9

Communications

Angew. Chem. Int. Ed. 2007, 46, 2444–2447

Coordination in the Gas Phase

DOI: 10.1002/anie.200604148

The Search for the Species with the Highest Coordination Number**

Andreas Hermann, Matthias Lein, and Peter Schwerdtfeger*

The question of the highest possible coordination number for an atom is addressed as this is related to the Gregory–Newton problem of kissing hard spheres.^[1] Using first-principles quantum chemical simulations we show that the interaction of Pb²⁺ with He atoms results in remarkably stable PbHe₁₅²⁺ with 15 atoms in the first coordination sphere forming a Frank–Kasper polyhedron.^[2] The Pb–He distances do not change significantly by subsequent filling of the first coordination shell as one expects for a hard-sphere model. Such high coordination numbers have been proposed only in liquid simulations so far.^[3]

The problem of how many spheres (N_{\max} , called the kissing number or Newton number) of a given radius R can be

conjunction with coordination numbers higher than 12 stabilized by the surrounding matrix.^[2]

Herein we take a different approach. We look for a single molecule MX_N in the gas phase of high coordination number N which can be experimentally verified. We choose a large positively charged central atom, M = Pb²⁺, and a very small ligand, X = He. Both atoms have reasonably small polarizabilities ($\alpha_{\text{He}} = 1.38 \text{ au}^{[10]}$ and $\alpha_{\text{Pb}^{2+}} = 14.1 \text{ au}^{[11]}$), and therefore fit the hard-sphere model quite well. The ionization potential of Pb⁺ (15.03 eV) is much smaller than that of He (24.58 eV).^[12] Hence, Pb²⁺–He does not undergo a Coulomb explosion and there is no (or minimal) charge transfer from He to Pb²⁺. Hence the Pb²⁺–He interaction $V(R)$ is mainly of

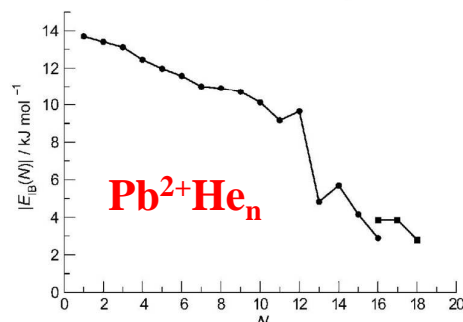
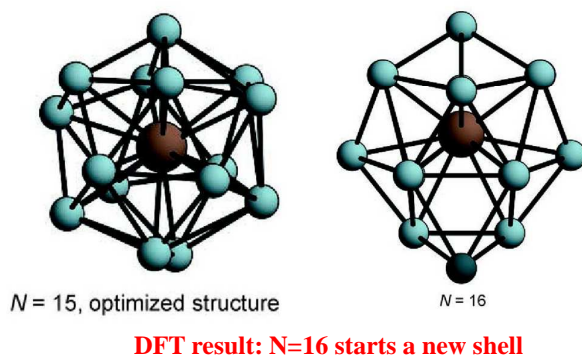


Figure 4. E_b for PbHe_N²⁺. Circles: minima of one-shell structures; squares: minima of two-shell structures.

Marius Lewerenz

Strasbourg, 12.7.2012

10

Modelling ions inside helium clusters

Alkali ions and **Pb²⁺** ions have closed electronic shells and an isotropic interaction potential with helium atoms.

Pb⁺ has an open shell s²p electronic configuration leading to **electronic anisotropy** and **X²Π** and **A²Σ⁺** states for **Pb⁺He**.

Similar systems of interest are **Ar⁺** ions (s²p⁵ valence shell, **X²Σ⁺** and **A²Π** states for **Ar⁺He**) and halogen atoms and ions interacting with helium, in particular **iodine**. Spin-orbit coupling between Σ and Π states has to be included in the model.

The road map:

Build reliable many body models for **He interacting with open shell species** by combining high level ab initio surfaces with accurate level predictions and comparison with spectroscopic or collision experiments.

Use an accurate quantum many body method for nuclear dynamics:

Diffusion quantum Monte Carlo (DMC)

Diffusion quantum Monte Carlo (DMC)

- Isomorphism between **time dependent Schrödinger equation** and a **multi dimensional diffusion equation** (Fermi, Ulam)
- Exact solution except for statistical errors

$$i\hbar \frac{\partial \Psi(\vec{r}, t)}{\partial t} = \left\{ -\frac{\hbar^2}{2} \sum_{j=1}^n \frac{1}{m_j} \nabla_j^2 + \{ \textcolor{red}{V}(\vec{r}) - E_{ref} \} \right\} \Psi(\vec{r}, t)$$

$$\frac{\partial C(\vec{r}, t)}{\partial t} = \left\{ \sum_{j=1}^n D_j \nabla_j^2 - \textcolor{red}{k}(\vec{r}) \right\} C(\vec{r}, t) .$$

Solution by propagation of an ensemble of random walkers in imaginary time
Cartesian coordinates, precision $\sigma_E/E = 10^{-6} - 10^{-3}$

DMC calculations for Ar^+He_n

Potential model:

Anisotropy due to Ar^+ s^2p^5 valence shell $\rightarrow \mathbf{X}^2\Sigma^+$ and $\mathbf{A}^2\Pi$ states for Ar^+He .

$\text{IP}(\text{Ar})=15.76 \text{ eV} \rightarrow \text{He}^++\text{Ar}$ channel is unimportant, single configuration.
RCCSD(T) calculations with (aug)-cc-pVXZ basis sets (**MOLPRO**).

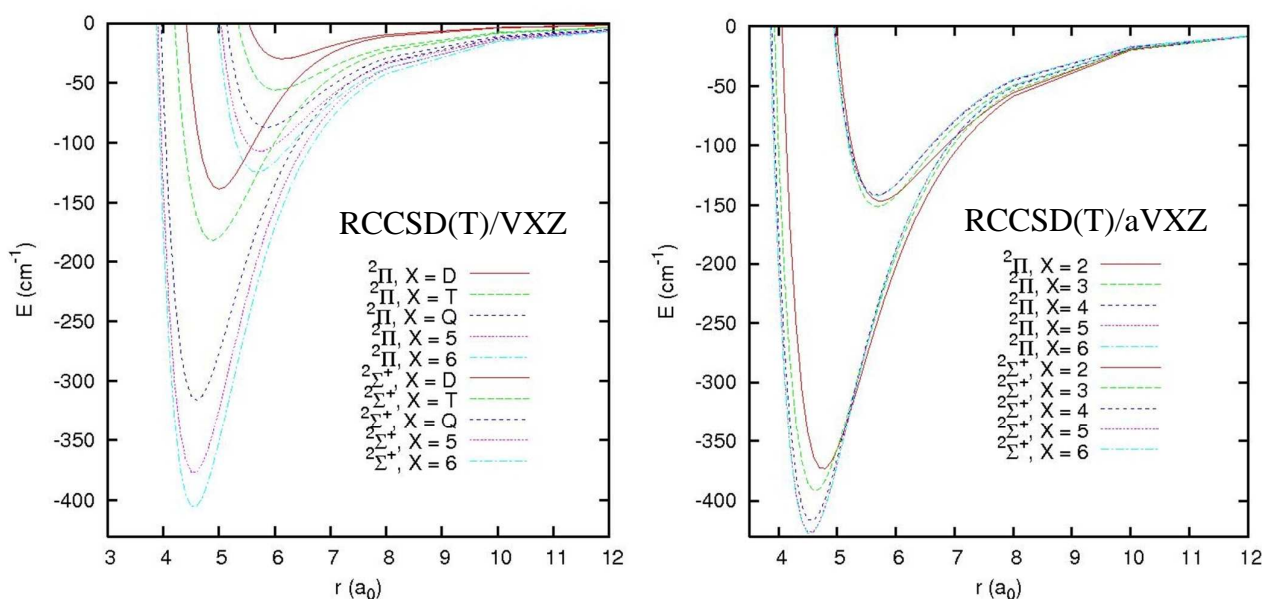
Infinite basis set ab initio points fitted to **HFD-style analytical form**
with fixed C_4 coefficient computed from $\alpha_{\text{He}} = 1.41 \text{ a}_0^3$.

Strong **spin-orbit interaction** in Ar^+ ($\Delta = 1432 \text{ cm}^{-1}$):

Non additive many body potential model including induced dipoles on He
with additional spin-orbit mixing included using atomic Δ_{Ar^+}
(**complex 6 x 6 matrix** to diagonalise in each DMC step).

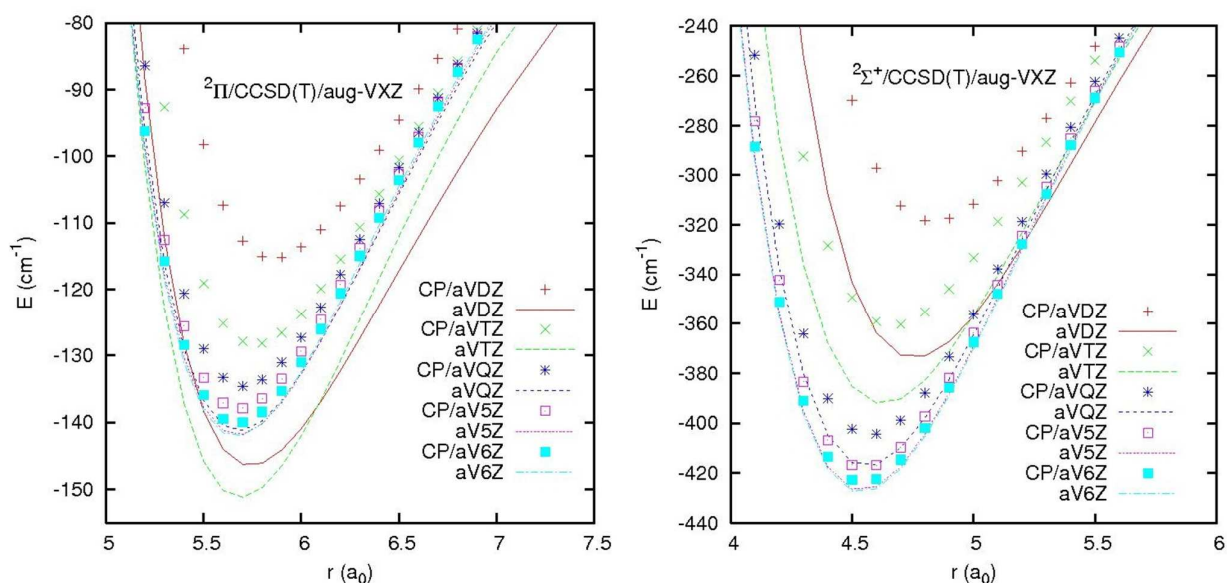
Ar^+He : convergence of interaction energy

RCCSD(T) calculation, standard and augmented basis sets



Ar⁺He: BSSE counter poise correction

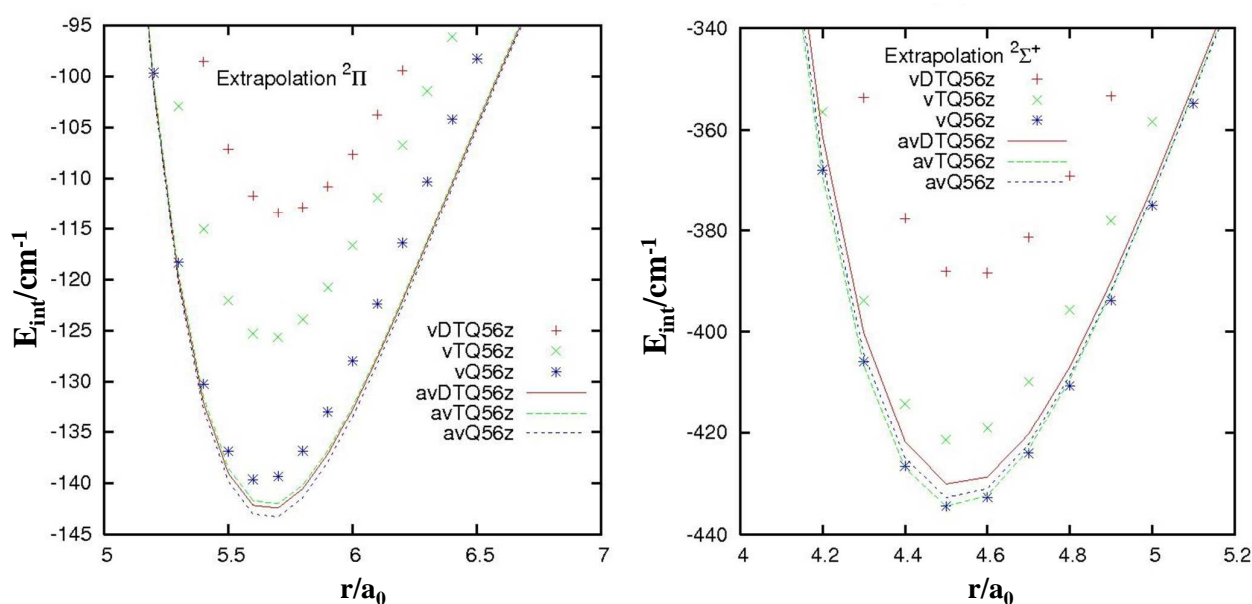
RCCSD(T) calculation



Unsatisfactory convergence for $^2\Pi$ state, $^2\Sigma^+$ looks ok but

Ar⁺He: basis set extrapolation

(aug)-cc-pVXZ series, SCF: exponential, RCCSD(T) correlation X⁻³



Augmented series is much more stable, remaining mismatch for $^2\Pi$ state

Ar⁺He: spectroscopic observables

extrapolated potentials (aQ56), atomic spin-orbit splitting,
variational rovibrational calculation in Laguerre basis, ⁴He⁴⁰Ar⁺

Vibrational transition frequencies in cm-1

v	$X\ ^2\Sigma_{1/2}^+$			$A_1\ ^2\Pi_{3/2}$		$A_2\ ^2\Pi_{1/2}$		
	exp	S96	This work	S96	This work	exp	S96	This work
0	92.9	83.9	92.47	52.9	55.91	69.2	64.0	69.19
1	66.2	55.2	64.88	26.9	29.20		35.1	38.82
2		30.7	38.55	11.9	11.73		15.7	17.59
3		14.1	17.81					

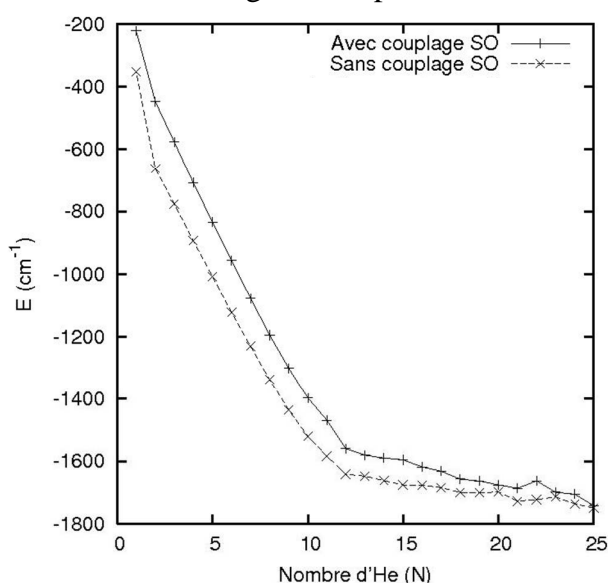
Expectation values for rotational constants in cm-1

0	0.659	0.614	0.650	0.460	0.469	0.515	0.501	0.514
1	0.551	0.518	0.559	0.355	0.365	0.420	0.397	0.412
2	0.39	0.404	0.450	0.241	0.255		0.282	0.298
3		0.282	0.324	0.168	0.087		0.182	0.180
4		0.182	0.196					

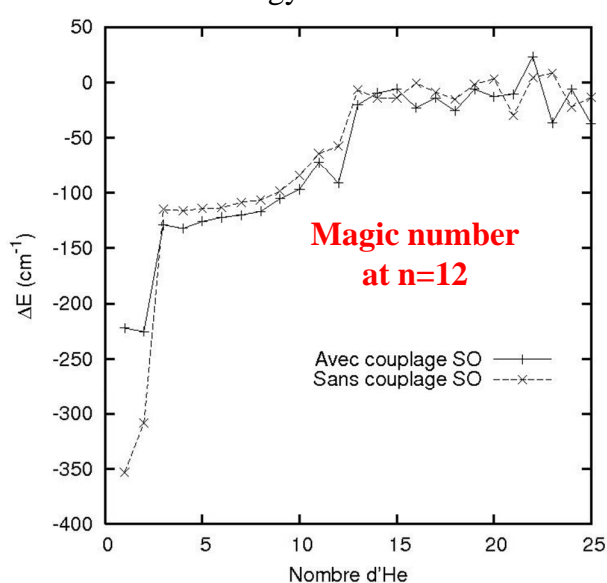
Our Ar⁺He potential is excellent !

Ar⁺He_n : DMC ground state energies

Total energies extrapolated to $\Delta\tau=0$



Energy increments



Spin orbit coupling is responsible for magic character of n=12 cluster

DMC calculations for $\text{Pb}^{q+}\text{He}_n$

$\text{Pb}^{2+}\text{He}_n$:

Isotropic Pb^{2+} - He interaction (Pb^{2+} s^2 valence shell, $\text{Pb}^{2+}\text{-He}$ $X^1\Sigma^+$).

Induced dipoles on He, He-dipoles induce a noticeable dipole on Pb^{2+} :

Non additive many body potential model checked against ab initio.

Pb^+He_n :

Anisotropy due to Pb^+ s^2p valence shell $\rightarrow X^2\Pi$ and $A^2\Sigma^+$ states for Pb^+He .

Strong **spin-orbit interaction** in Pb^+ ($\Delta = 14081 \text{ cm}^{-1}$):

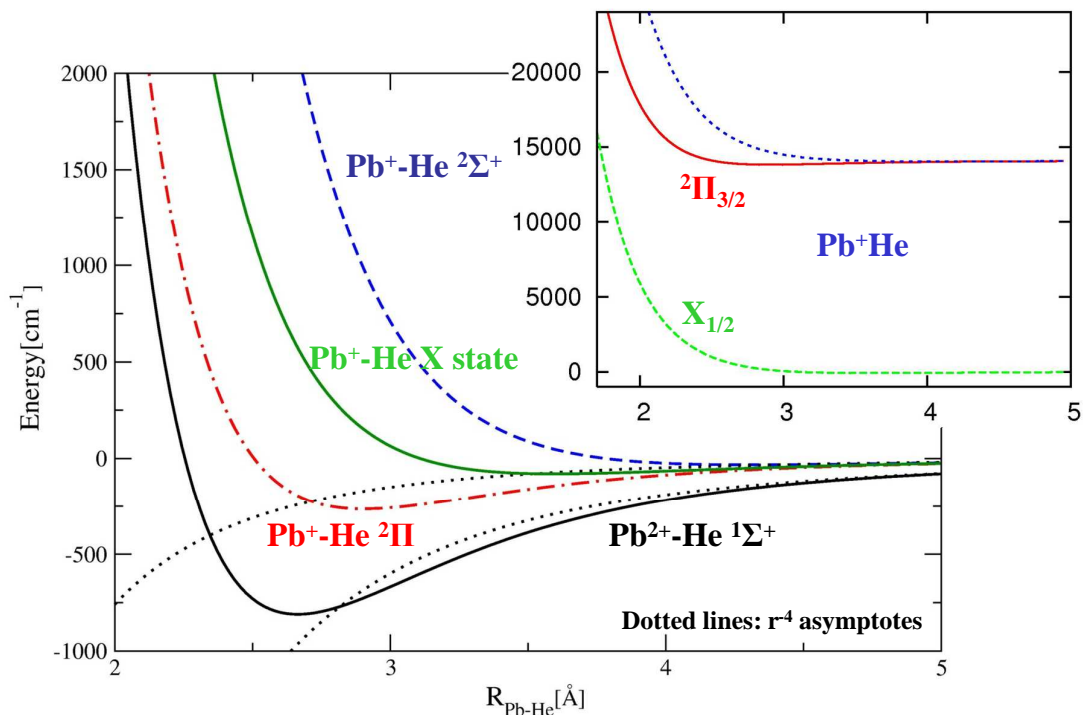
Non additive many body potential model including induced dipoles on He with additional spin-orbit mixing included using atomic Δ_{Pb^+}

(**complex 6 x 6 matrix** to diagonalise in each DMC step).

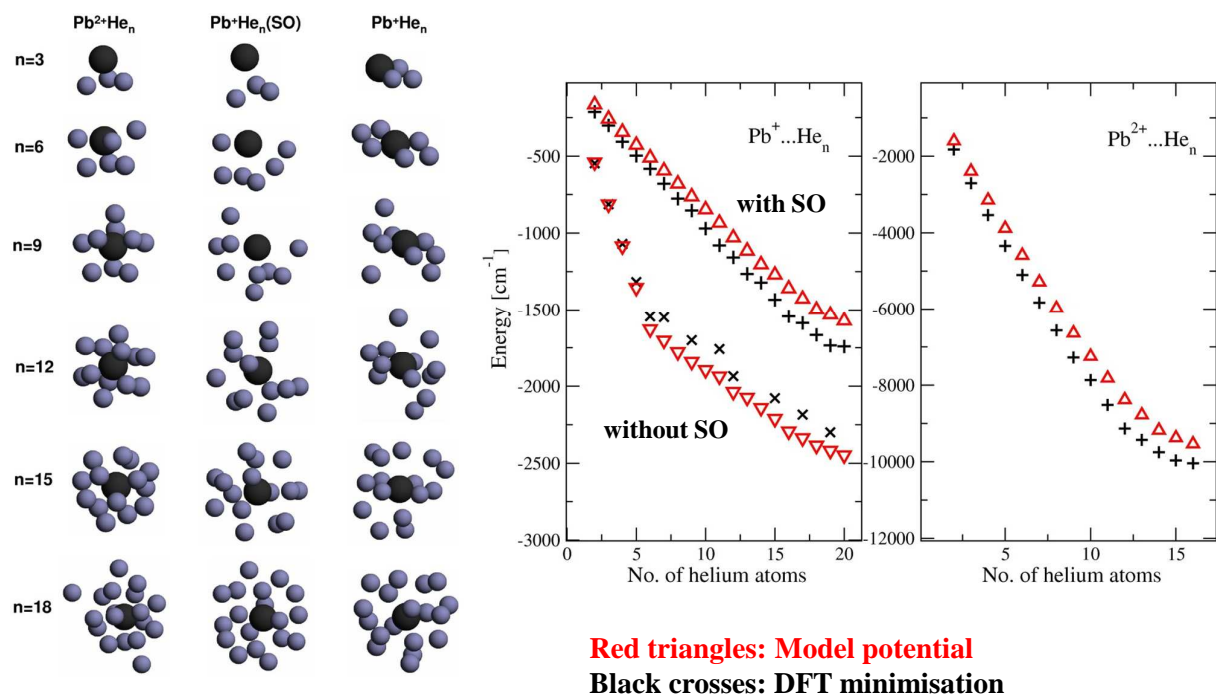
CCSD(T) calculations with Stuttgart pseudopotentials for both systems in collaboration with Petr Slavíček.

> 10^9 DMC samples, large ensemble sizes to suppress ensemble size bias

Pair interaction potentials for $\text{Pb}^{q+}\text{He}_n$



Minimum energy structures for Pb^q+He_n

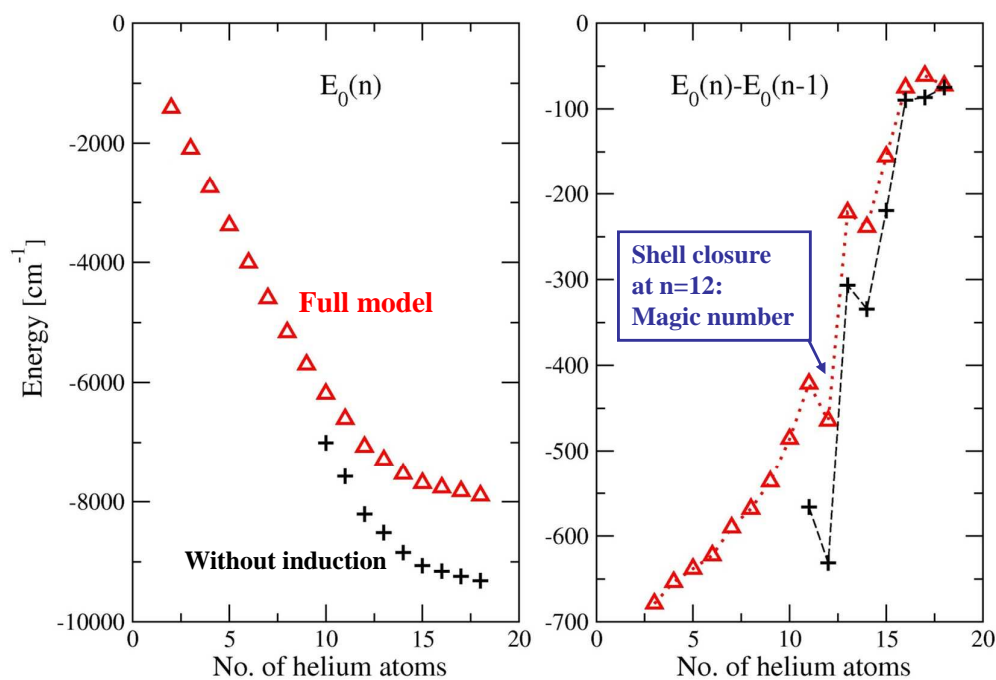


Marius Lewerenz

Strasbourg, 12.7.2012

21

DMC ground state energies for $\text{Pb}^{2+}\text{He}_n$

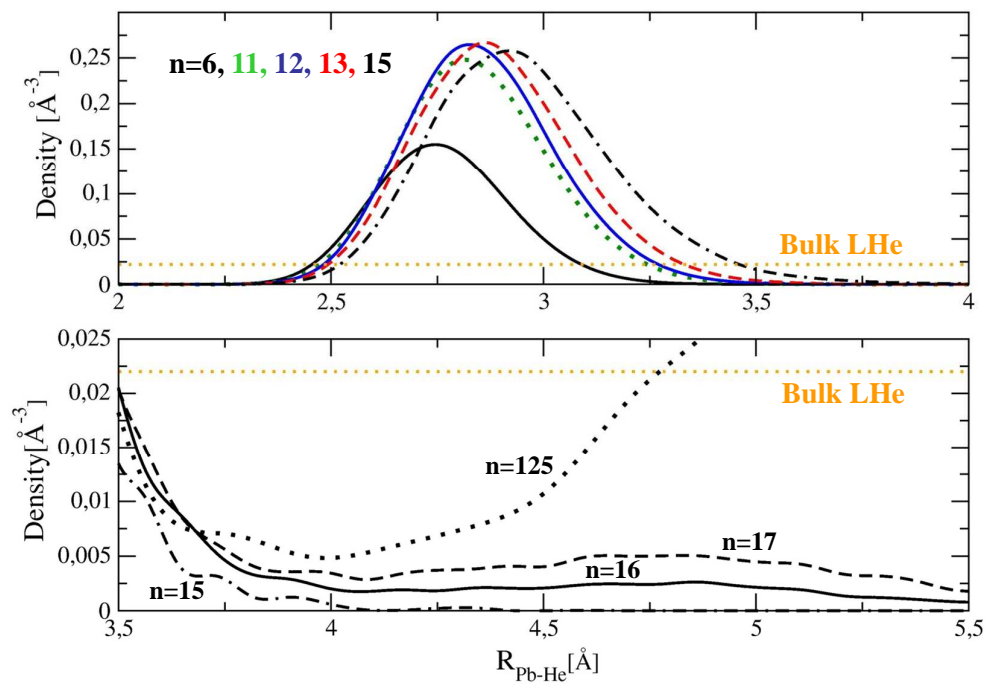


Marius Lewerenz

Strasbourg, 12.7.2012

22

Radial densities for $\text{Pb}^{2+}\text{He}_n$

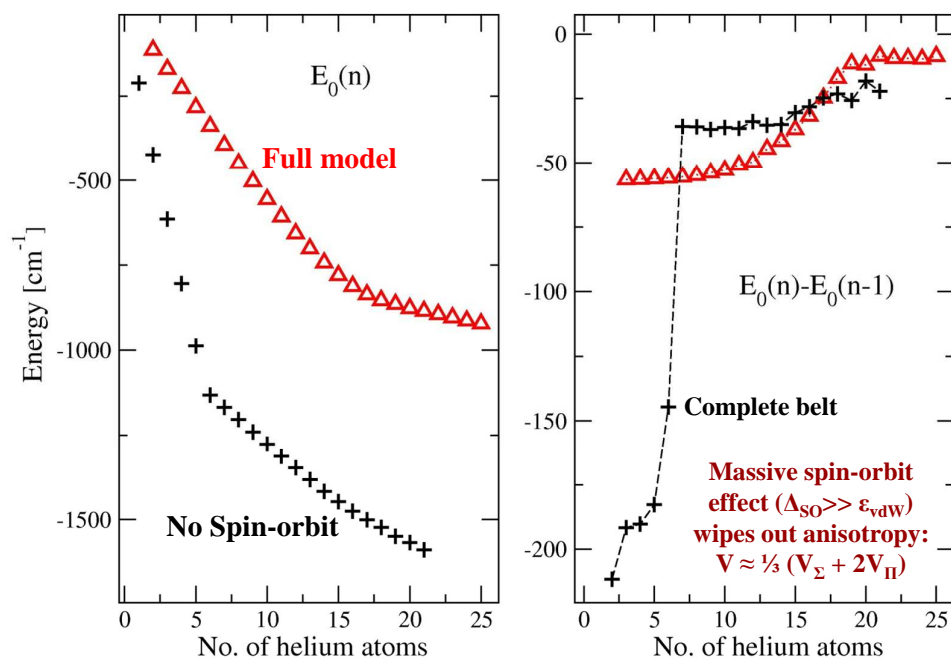


Marius Lewerenz

Strasbourg, 12.7.2012

23

Ground state energies for Pb^+He_n

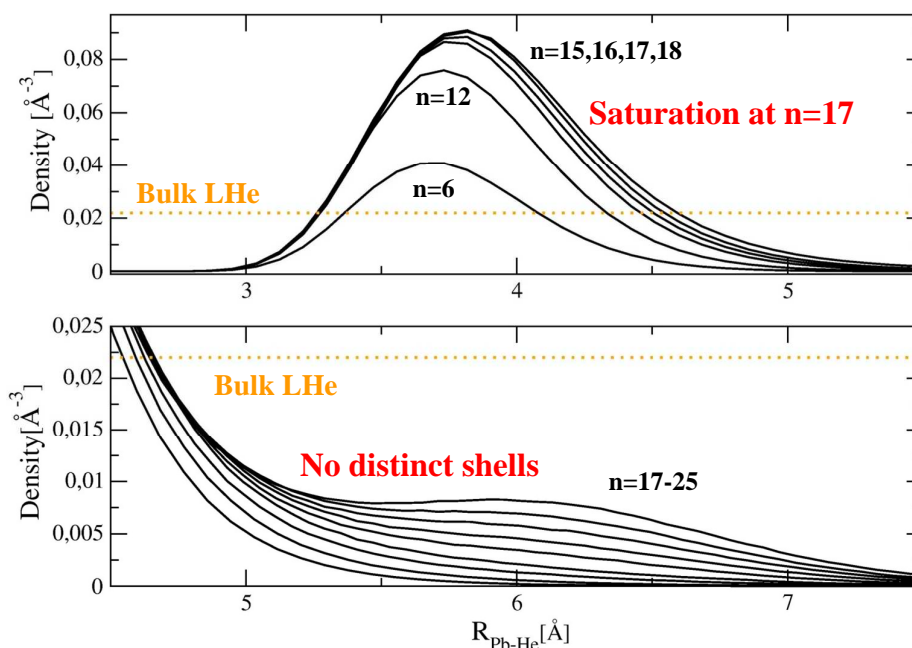


Marius Lewerenz

Strasbourg, 12.7.2012

24

Radial densities for Pb^+He_n



DMC calculations for I@He_n

Motivation: Photodissociation of $\text{CH}_3\text{I} \rightarrow \text{CH}_3 + \text{I}$ inside He_n .

We need global potential energy surfaces for ground and excited $\text{CH}_3\text{I@He}_n$ and for the relevant fragments $\text{CH}_3\text{@He}_n$ and I@He_n

Potential model:

Anisotropy due to I s^2p^5 valence shell $\rightarrow \text{X}^2\Sigma^+$ and $\text{A}^2\Pi$ states for I-He.
RCCSD(T) calculations with aug-cc-pVXZ basis sets and relativistic pseudopotential (**ECP**) from K. Petersen.

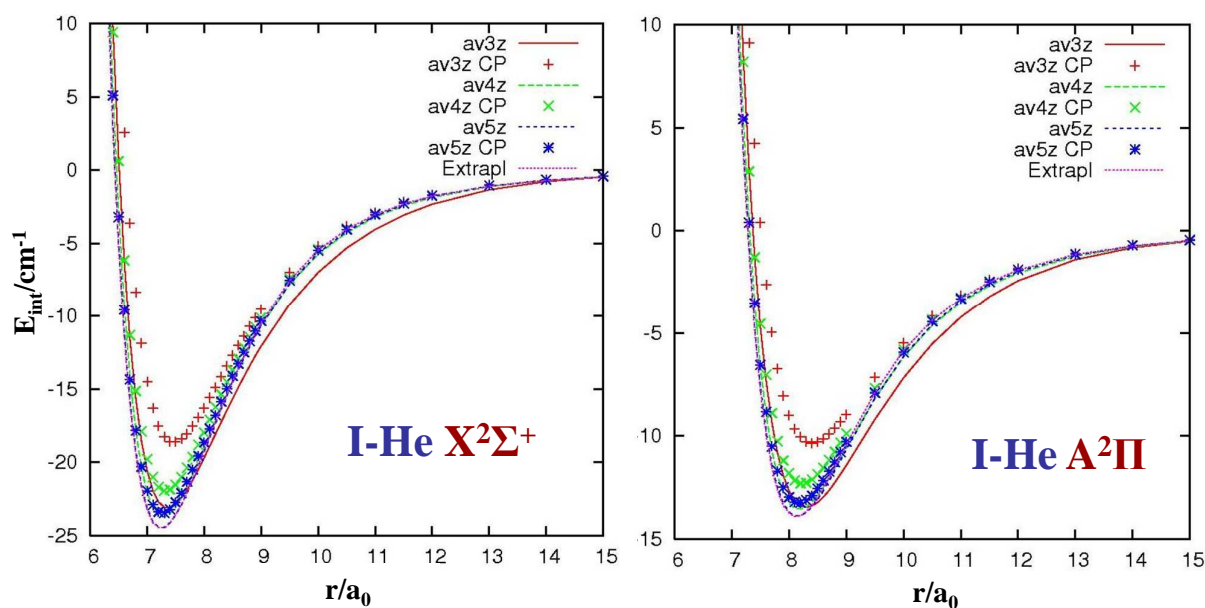
Ab initio points fitted to **extended Tang-Toennies** analytical form.

Very strong **spin-orbit interaction** in I:

Non additive many body potential model with additional spin-orbit mixing using atomic Δ_{I} (**complex 6 x 6 matrix** to diagonalise in each DMC step).

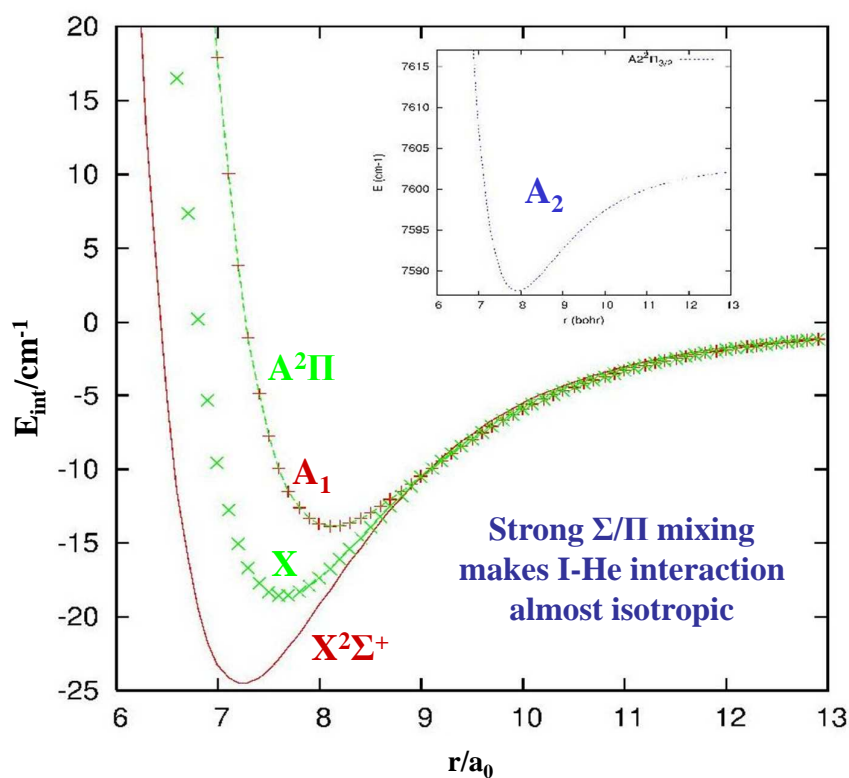
Δ_{SO} dominates so much over E_{vdW} that SO mixing is almost perfect!

I-He: Convergence of RCCSD(T)/ECP calculations

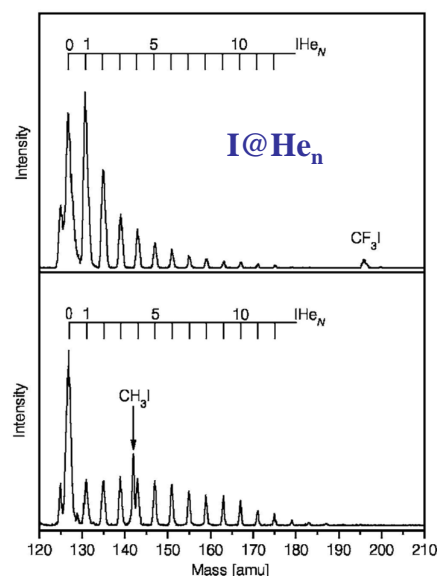
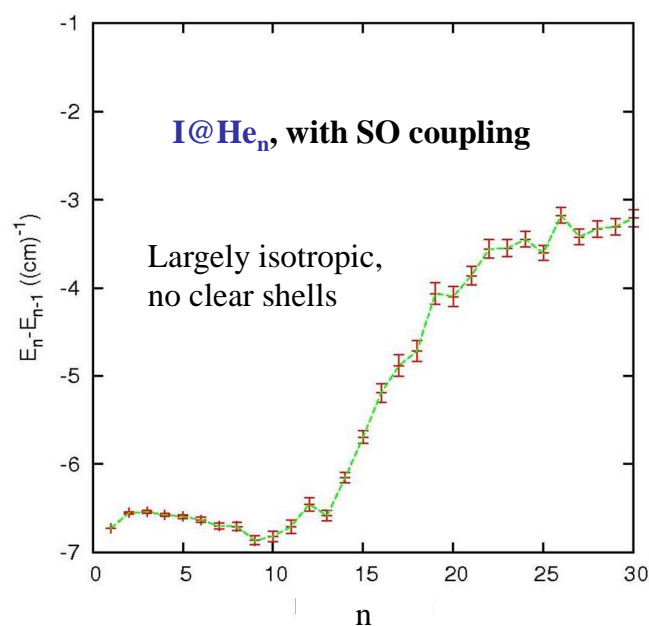


Spin-orbit coupling mixes the $^2\Sigma_{1/2}$ and $^2\Pi_{1/2}$ components: 6x6 complex matrix

I-He: Interaction potential with SO coupling

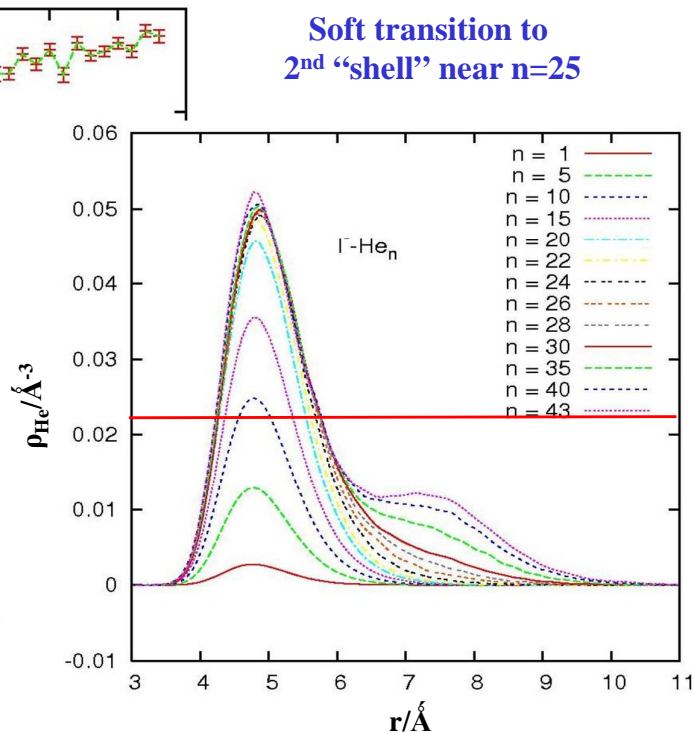
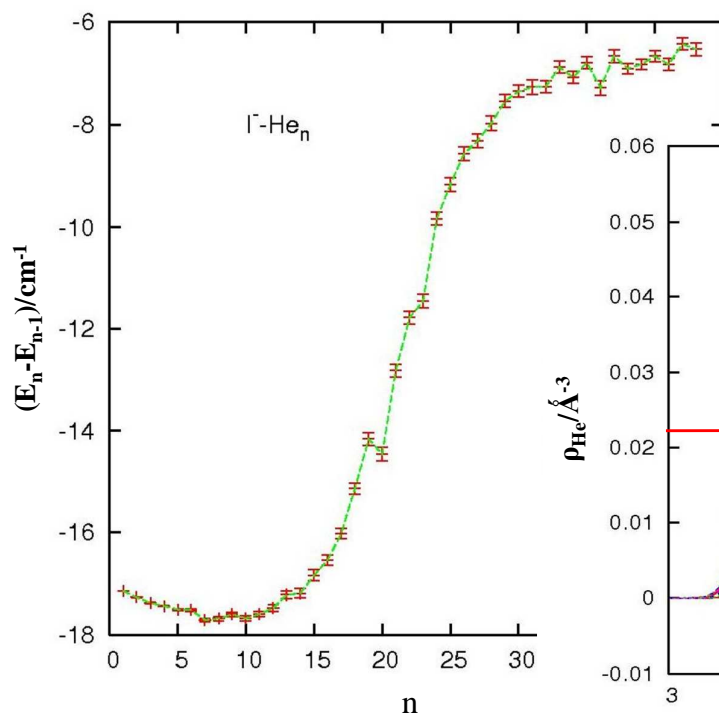


I@He_n: Incremental binding energies from DMC

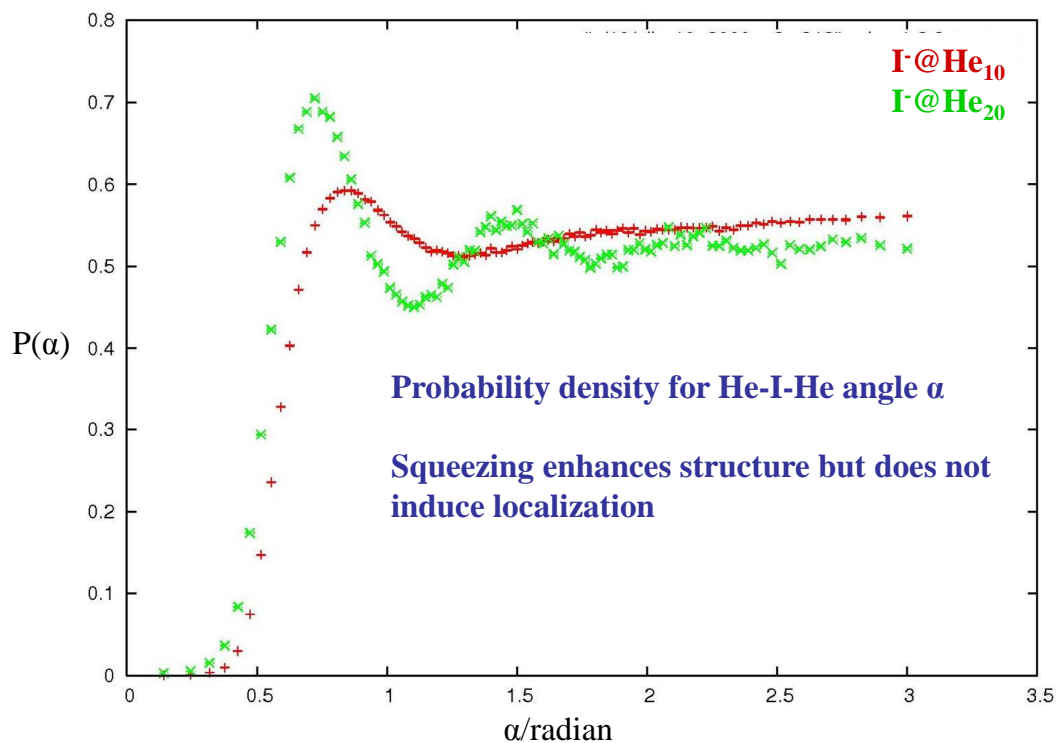


Braun and Drabbels 2007

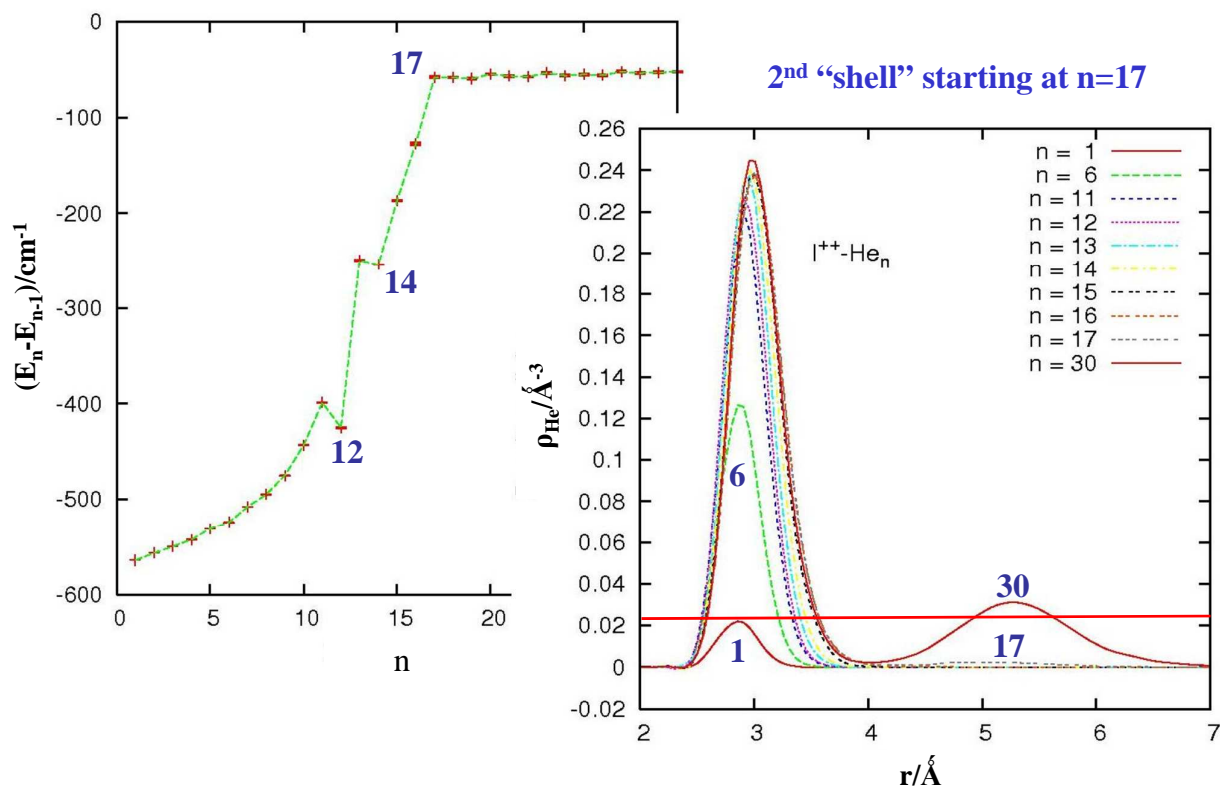
I⁻@He_n: Binding energy and radial helium density



I⁻@He_n: Angular correlations



I²⁺@He_n: Binding energy and radial helium density



CO⁺-He and CO⁺@He_n

CO⁺He ions have been observed several times in drift tube experiments.

Mixed cluster ions of the composition CO⁺He_n should be accessible in drift tube experiments, mixed gas expansions coupled to electric discharges, or CO ionization inside large He clusters.

Ionisation of CO barely changes the rotational constants but strongly affects the interaction with helium: CO@He_n and CO⁺He_n are an ideal pair to understand **rotation in helium clusters** by separating effects due to mass and interaction.

Potential surface can be checked by ion depletion spectroscopy (see N₂⁺-He_n).

Astrophysical motivation

CO is a relatively abundant molecule in interstellar space and CO⁺ has been identified in 1993. Low energy collisions with its second most abundant collision partner, helium atoms, are governed by the weak intermolecular interaction leading to the van der Waals complex He-CO⁺.

Interaction and structure, what to expect?

Electrostatics/induction:

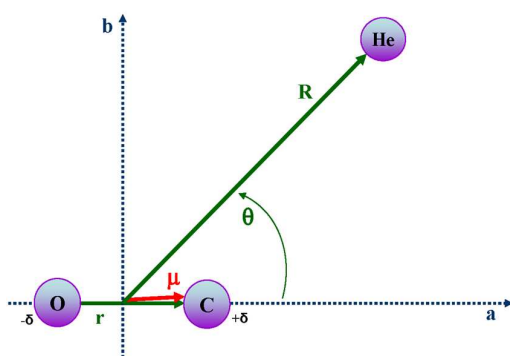
Charge – induced dipole: isotropic $\sim 1/R^4$

Permanent dipole – induced dipole: anisotropic $\sim 1/R^5 \rightarrow$ linear complex

Quadrupole moment – induced dipole: anisotropic $\sim 1/R^6 \rightarrow$ T-shaped

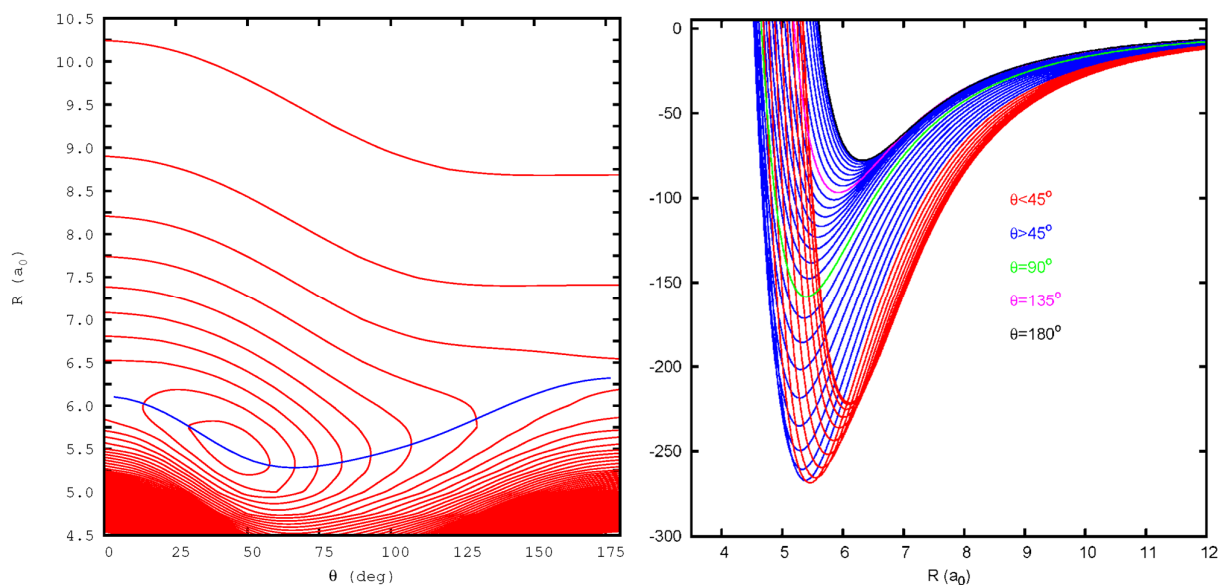
Dispersion: anisotropic $\sim 1/R^k$, $k \geq 6$

Result: Compromise between linear and T-shaped at short range,
linear long range approach: **Floppy, quasilinear?**



Ab initio CCSD(T) equilibrium structure of He-CO⁺(X²Σ⁺) and the dipole moment vector μ .

Features of the CO⁺-He surface



2D contour plot of the RCCSD(T) PES.

Contour lines at intervals of 25 cm⁻¹, first contour placed at -250 cm⁻¹. The blue line shows the variation of the Jacobi distance R along the minimum energy path in the direction of the Jacobi angle θ .

Radial cuts for several values of the Jacobi angle θ .

Marius Lewerenz

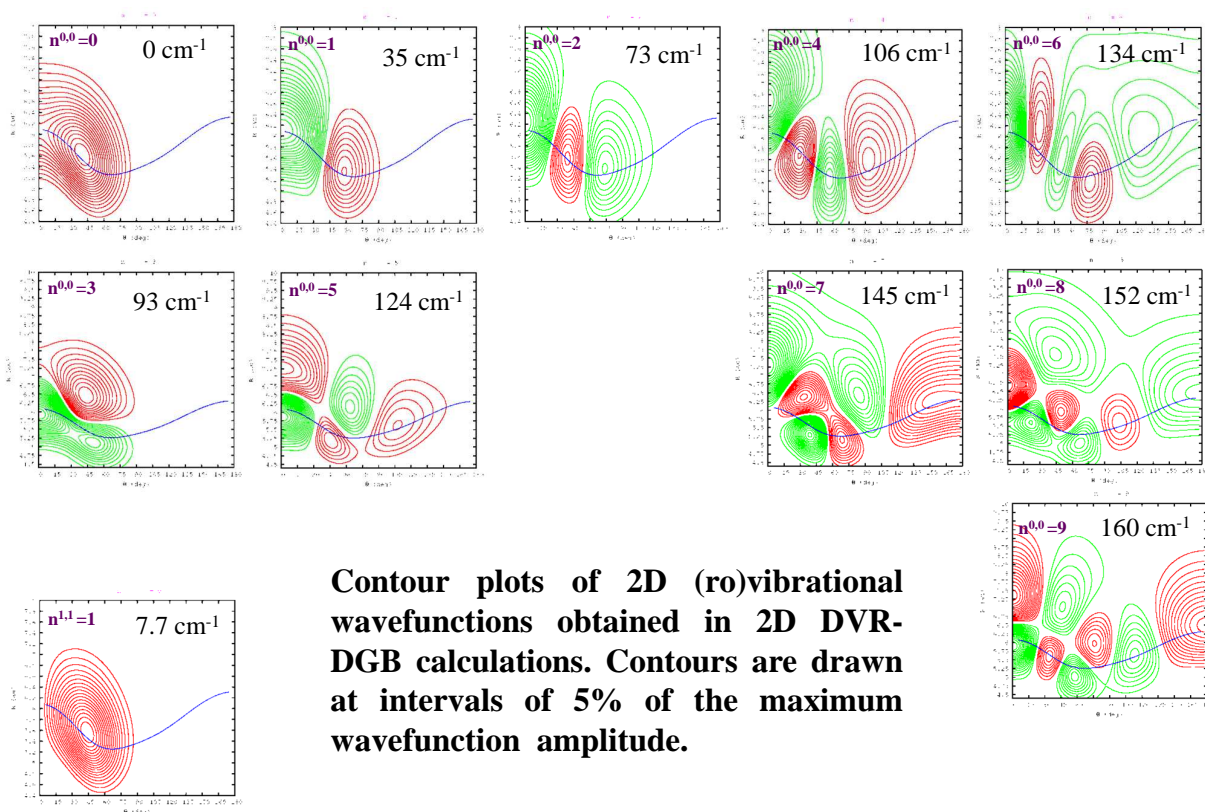
Strasbourg, 12.7.2012

35

Spectroscopic results from DVR-DGB calculations

He-CO⁺(X² Σ^+) 2D RCCSD(T) potential energy surfaces V(R, θ) at r(CO)=1.11783 Å

	avtz	avtz _{corr}	avqz	avqz _{corr}	av5z	av5z _{corr}	av ∞ z
$R_e/\text{\AA}$	2.898	2.905	2.870	2.878	2.868	2.871	2.866
θ_e/deg	43.8	46.2	45.8	46.0	46.1	46.1	46.3
V_{min}/cm^{-1}	-285.8	-252.4	-281.6	-269.0	-277.7	-274.0	-275.3
E_0/cm^{-1}	-209.7	-177.5	-201.3	-189.9	-197.6	-194.2	-195.0
A_0/cm^{-1}	10.3	7.315	7.679	7.328	7.362	7.256	7.168
B_0/cm^{-1}	0.444	0.454	0.462	0.462	0.465	0.465	0.466
C_0/cm^{-1}	0.395	0.400	0.408	0.407	0.410	0.409	0.411
ν_2/cm^{-1}	31.9	32.8	34.3	34.4	34.7	34.7	34.9
ν_3/cm^{-1}	94.8	86.5	94.2	91.3	93.6	92.8	93.3
Δ_1/cm^{-1}	0.049	0.055	0.056	0.055	0.055	0.055	0.056
κ	-0.990	-0.984	-0.985	-0.984	-0.984	-0.984	-0.983
γ_0	-0.31	0.08	0.08	0.12	0.12	0.14	0.15



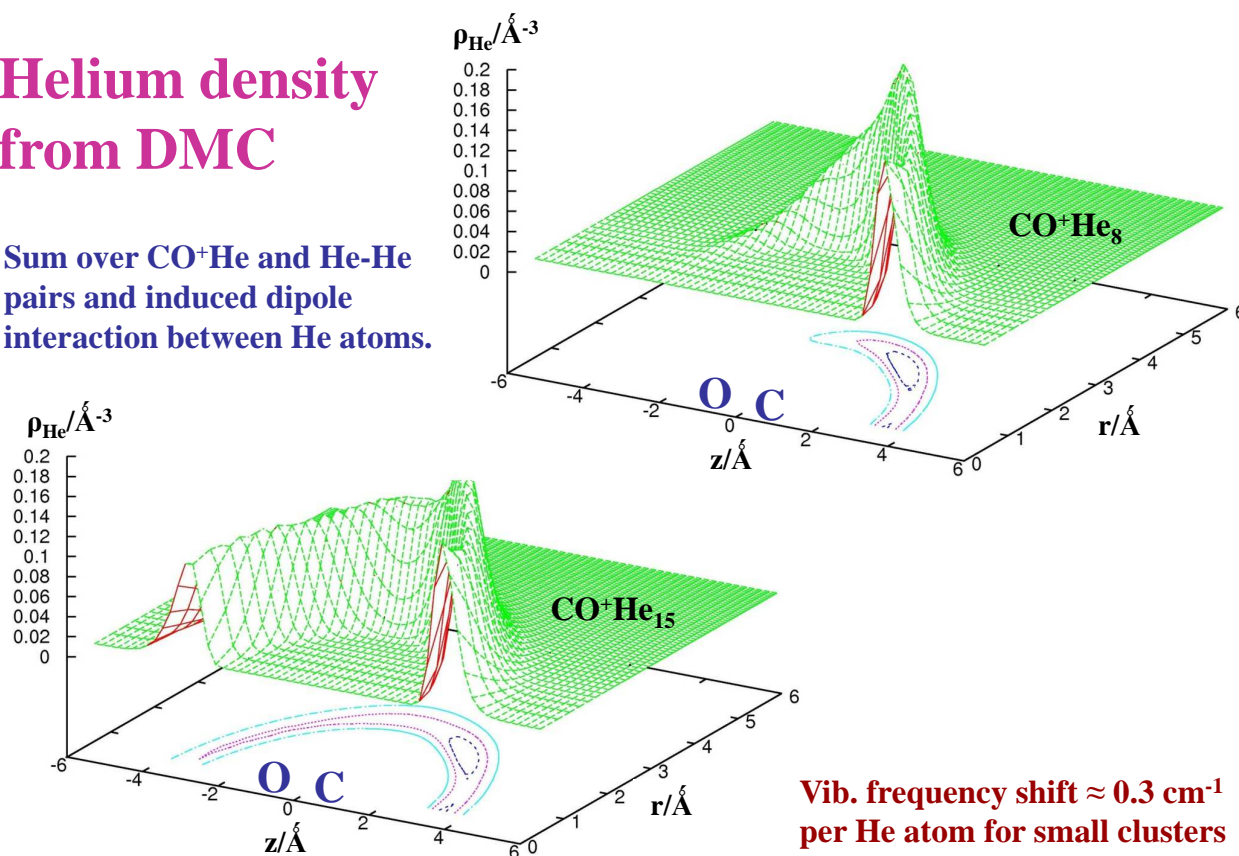
Marius Lewerenz

Strasbourg, 12.7.2012

37

Helium density from DMC

Sum over CO⁺He and He-He pairs and induced dipole interaction between He atoms.

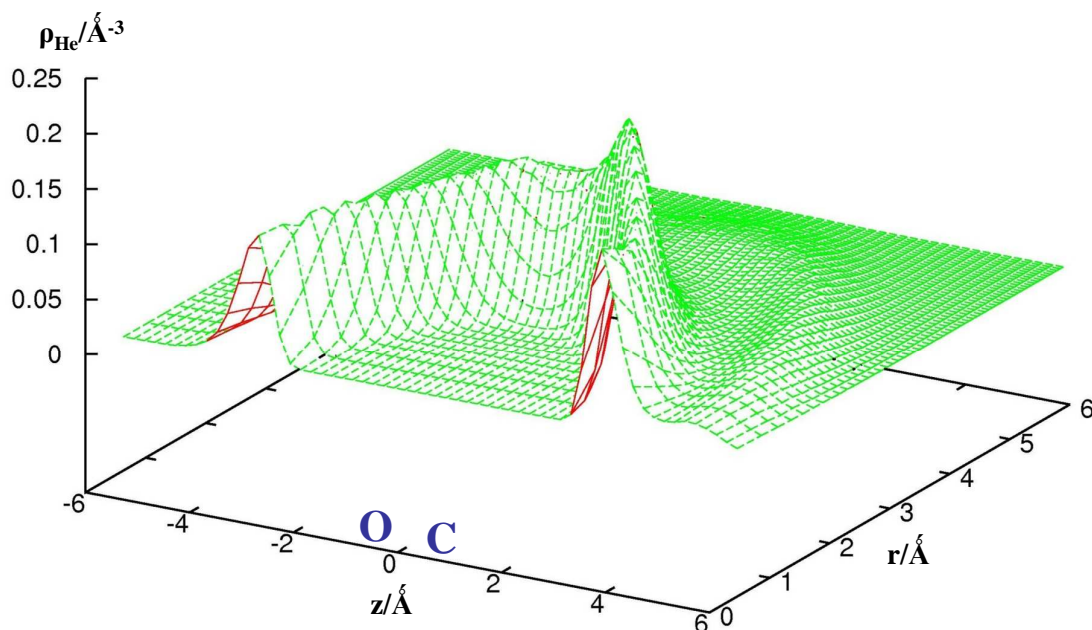


Marius Lewerenz

Strasbourg, 12.7.2012

38

CO⁺@He₂₀: helium density from DMC



CH₃-He

- Ab initio **RCCSD(T)** calculations with **aug-cc-pVXZ** basis sets (**X=D,T,Q,5**)
- **CH₃** keeping **C_{3v}** symmetry and fixed C-H distance: only **umbrella angle α**
- **He** position relative to **CH₃** center of mass in **spherical coordinates R, θ, ϕ**
- Several 3D surfaces assembled into 4D surface including **CH₃** relaxation
- Overall about 3000 potential energy points

Analytical representation with **angle dependent HFD** form expanded over real spherical harmonics T_{lm} with symmetry restrictions on l, m :

$$V(R, \theta, \phi) = A \exp\{-b(\theta, \phi) [R - R_e(\theta, \phi)]\} - \sum_k C_k(\theta, \phi) / R^k$$

$$X(\theta, \phi) = \sum_{lm} x_{lm} T_{lm}(\theta, \phi) \quad X = b, R_e, C_k$$

500-1000 points per 3D cut are fitted with 38 parameters and rms < 0.1 cm⁻¹

Outlook

- Vibrational shifts and effective rotational constants for CO^+ in helium (DMC/PIMC in collaboration with P. N. Roy).
- CH_3 radicals in helium, reactive complexes.
- Photodissociation of CH_3I and CF_3I (ZPAD, DMC etc.)
- Dopant spectroscopy (Mg^* , Ag^* , Ag^+ etc.).
- Transport properties (Mg^+ , Na^+).
- DMC and ZPAD calculations on Xe_nHe_m .
- DMC with constraints ($(\text{H}_2)_n$, $\text{He}_n(\text{H}_2)_m$ possible).
- SBDMC: soft body DMC allowing feedback between dopant and bath vibrations

ANR project DYNHELIUM (Toulouse, Rennes, Paris)